Ecological Archives E096-139

Weintraub, S. R., P. G. Taylor, S. Porder, C. C. Cleveland, G. P. Asner and A. R. Townsend. 2015. Topographic controls on soil nitrogen availability in a lowland tropical forest. *Ecology* 96:1561-1574.

Appendix A: Explanatory text, equations, a table, and two figures related to the nitrogen stable isotope mass balance modeling, as well as four additional tables containing soil chemical and physical data from the study site.

Nitrogen Isotope Mass Balance Modeling

We employed steady-state ^{15}N mass balance models (following Brenner et al. 2001, Amundson et al. 2003, and Hilton et al. 2013) to explore whether increased non-fractionating N losses (i.e. particulate nitrogen erosion) could explain observed soil N isotopic variation with changes in slope angle. According to these steady-state models, the $^{15}N/^{14}N$ ratio of soils (R_s) is modified from the mean weighted isotopic ratio of inputs (R_{in}) by a bulk or apparent ecosystem fractionation factor (α_{ex}):

$$R_s = R_{in} / \alpha_{ex} \quad \text{(A.1)}$$

In turn, α_{ex} is determined by the relative proportions of the soil N rate loss constant (k_{ex}) that are comprised of fractionating (k_f) and non-fractionating (k_E) pathways, as well as their fractionation factors, α_f and α_E respectively:

$$\alpha_{ex} = \alpha_f*(k_f/k_{ex}) + \alpha_E*(k_E/k_{ex}) \qquad \text{(A.2)}$$

Since N inputs and losses must be equal to satisfy N mass balance under steady state conditions, k_{ex} can be estimated from the total soil N content (N_s) and the rate of new N input (I):

$$k_{ex} = I/N_s \text{ (A.3)}$$

We used parameter values from our study site and the literature (Table A5) to explore several model scenarios. In the first three scenarios (A, B, and C in Fig. A1), we assigned all N inputs to the atmosphere, with R_{in} = 0.0036765. For scenarios A and B, we assumed there was a trade-off between N loss pathways, such that k_E and k_f varied inversely but with no change in total N loss (k_{ex}) at a given location. The difference between the two scenarios was that in A, we assigned invariant N_s values regardless of k_E (mean 0–10 cm soil N content across the Piro toposequence), while in B we allowed N_s values to decline as k_E increased. The latter was based on our observations of large, linear declines in N_s with increases in slope angle across the Piro toposequence. We estimated α_f using our data (Table A5) and assumed a constant α_f across the landscape. By definition, α_E was set to 1.

For scenarios A and B, a decline in $\delta^{15}N$ values from ~ 6.8 to 3.8 ‰, similar to what we observed from flat to steeply sloping terrain, could be simulated with an increase in k_E from 0 to 1.7 and 2.1 x 10^{-3} yr^{-1} (respectively), and in k_E/k_{ex} from 0 to 0.45 (Fig. A1a). These absolute values of k_E translate to an increase from 0 to 4.5 kg N ha^{-1} yr^{-1} lost by non-fractionating pathways (Fig. A1b). The shape of the curve for scenario A is more similar to observed data, but scenario B is arguably more realistic. As such, we chose to apply N_s values from scenario B to subsequent modeled scenarios.

In scenario C, we relaxed our assumption of a strict trade-off between fractionating and non-fractionating loss pathways, akin to Hilton et al. (2013). In this case, we allowed equal magnitudes of fractionating losses to persist across the landscape but non-fractionating losses to increase on slopes, resulting in variable k_{ex} across the landscape. Using similar parameter values as above (Table A5) but allowing k_f to remain constant while k_E increased and N_s decreased, the observed shift in $\delta^{15}N$ values was reproduced as k_E/k_{ex} increased from 0 to 0.45. This translated to a larger absolute increase in k_E compared to scenarios A and B (from 0 to 2.6 x 10^{-3} yr^{-1}, Fig. A1a), or an increase from 0 to 6 kg ha^{-1} yr^{-1} of non-fractionating N loss from gentle to steep terrain (Fig. A1b). While this is not an unreasonable estimate, and some measurements from our site may lend support for this scenario (such as similar N_2O fluxes from ridge and slope), the predicted total increase in k_{ex} – from 3.6 to 6.7 x 10^{-3} yr^{-1} – necessitates a large parallel increase in N inputs to satisfy N mass balance under steady-state conditions. While it is possible that N inputs do increase on steep slopes, a near-doubling seems unlikely, especially given preliminary free-living N fixation rates measured along the toposequence (S. Weintraub, *unpublished data*). Therefore, similar to Hilton et al. (2013), we suggest that a trade-off between fractionating and non-fractionating losses across the landscape is the more likely scenario.

Finally, the weathering of N-bearing sedimentary rocks can impact soil isotopic composition as bedrock $\delta^{15}N$ values are likely to be distinct from atmospheric sources (Holloway and Dahlgren 2002, Morford et al. 2011). We do not know the N content or isotopic composition of southern Osa greywackes, but we used mass balance models to explore how changes in the mean weighted isotopic ratio of inputs (R_{in}), which would occur with variable proportions of N inputs from atmospheric (I_A/I) and bedrock (I_r/I) sources, affect R_s. The mean weighted isotopic ratio of inputs is dependent on the relative proportions of N input pathways and their respective $^{15}N/^{14}N$ ratios:

$$R_{in} = R_A*(I_A/I) + R_r*(I_r/I) \quad (A.4)$$

In these "rock N" scenarios, we allowed I_r/I to increase linearly with slope angle. Since R_r values were assumed to be higher then the atmosphere, this caused R_{in} to increase. We assumed a tradeoff between I_A and I_r such that total N inputs were invariant, which seemed reasonable since the energetically expensive process of biological N fixation should be down-regulated when other N sources are available. As above, we also imposed a tradeoff between k_E and k_f. We explored the affects of variable amounts of rock N input on k_E/k_{ex} and $\delta^{15}N$ across a range of increasing I_r/I values and a range of rock $\delta^{15}N$ values (1 to 6 ‰) based on the literature.

Results from these rock N scenarios reveal a positive linear relationship between bedrock N inputs (I_r/I) and non-fractionating N losses required to achieve N mass balance (Fig. A2). The coefficients of linear relationships depend strongly on rock $\delta^{15}N$; absolute values of k_E/k_{ex} and k_E on the steepest slopes vary from 0.48 to 0.88 and 2.3 to 4.3 x 10^{-3} respectively (Fig. A2a). This translates to PN losses that increase from between 4.5 to 8.5 kg N ha^{-1} yr^{-1} along the transition from gentle to steeply sloping terrain (Fig. A2b). Rock N inputs cannot be ruled out based on isotope data, as this range of predicted PN losses is possible at the study site. However, large I_r/I values (> 25%) and high rock $\delta^{15}N$ values (> 2‰) require very large increases in k_E along local slope gradients in order to achieve observed isotope patterns. Dominance by non-fractionating losses is increasingly required to model ^{15}N dynamics across the landscape if rock N plays an important role. Contributions of rock N that are small and/or have low $\delta^{15}N$ values are easier to reconcile with the data and the geomorphology of this region.

LITERATURE CITED

Amundson, R., A. T. Austin, E. A. G. Schuur, K. Yoo, V. Matzek, C. Kendall, A. Uebersax, D. Brenner, and W. T. Baisden. 2003. Global patterns of the isotopic composition of soil and plant nitrogen. Global Biogeochemical Cycles 17 doi:10.1029/2002GB001903.

Brenner, D., R. Amundson, W. T. Baisden, C. Kendall, and J. Harden. 2001. Soil N and ^{15}N variation with time in a California annual grassland ecosystem. Geochimica et Cosmochimica Acta 65:4171–4186.

Dentener, F., J. Drevet, J. F. Lamarque, I. Bey, B. Eickhout, a. M. Fiore, D. Hauglustaine, L. W. Horowitz, M., et al. Nitrogen and sulfur deposition on regional and global scales: A multimodel evaluation. Global Biogeochemical Cycles 20: doi:10.1029/2005GB002672.

Hilton, R. G., A. Galy, A. J. West, N. Hovius, and G. G. Roberts. 2013. Geomorphic control on the δ^{15}N of mountain forests. Biogeosciences 10:1693–1705.

Holloway, J. M., and R. A. Dahlgren. 2002. Nitrogen in rock: Occurrences and biogeochemical implications. Global Biogeochemical Cycles 16 doi:10.1029/2002GB001862

Morford, S. L., B. Z. Houlton, and R. A. Dahlgren. 2011. Increased forest ecosystem carbon and nitrogen storage from nitrogen rich bedrock. Nature 477:78–81.

Sullivan, B. W., W. K. Smith, A. R. Townsend, M. K. Nasto, S. C. Reed, R. L. Chazdon, and C. C. Cleveland. 2014. Spatially robust estimates of biological nitrogen (N) fixation imply substantial human alteration of the tropical N cycle. Proceedings of the National Academy of Science 111:8101–8106.

Table A1. Mean values with standard errors in parentheses of eight soil N cycle metrics along the toposequence. Values are from surface soils, 0-20 cm. Letters indicate significant differences between positions according to Bonferroni-adjust *P* values ($\alpha = 0.05$).

	$\delta^{15}N$ (‰)	NO_3^- (ug N/g)	NH_4^+ (ug N/g)	Net nitrification (ug N/g/d)	Net N min (ug N/g/d)	Net nit: net N min	Nitrification Potential (ug N/g/d)	N_2O (ng N/ cm^2/hr)
Ridge	6.22[a] (0.12)	1.78[a] (0.25)	3.93[a] (0.23)	0.33[a] (0.09)	0.23 (0.11)	2.12 (0.76)	10.12[a] (2.10)	0.578 (0.034)
Shoulder	6.43[a] (0.13)	0.20[b] (0.03)	2.56[b] (0.17)	0.09[b] (0.03)	-0.07 (0.10)	0.48 (0.40)	1.61[b] (0.27)	0.380 (0.089)
Slope	5.07[b] (0.23)	0.13[b] (0.03)	2.33[b] (0.16)	0.01[b] (0.02)	0.07 (0.10)	0.01 (0.17)	1.53[b] (0.48)	0.484 (0.078)
F	19.69	57.14	17.59	13.71	2.27	4.56	20.77	2.54
P	<0.0001	<0.0001	<0.0001	0.0002	0.1354	0.0170	<0.0001	0.1068
P_{Bon}	0.0002	<0.0001	0.0005	0.0027	1.0000	0.1365	0.0002	0.8548

Note: Numerator degrees of freedom equals two for all statistical tests. Denominator degrees of freedom equals 18 for all tests except net nitrification, net N mineralization, and net nitrification: net N mineralization, which have 16 denominator degrees of freedom. P_{Bon} was calculated by multiplying by the number of comparisons (i.e., 8).

Table A2. Soil carbon and nitrogen concentrations and stocks along the toposequence and with depth. Stocks were calculated using bulk density values presented in Table A3.

Sample ID	Depth (cm)	Soil C (%)	Soil N (%)	Soil C (kg/m^2)	Soil N (kg/m^2)
Ridge 1	20	3.77	0.40	5.02	0.53
Ridge 1	40	2.49	0.23	4.03	0.38
Ridge 1	60	1.58	0.15	2.67	0.26
Ridge 1	80	1.24	0.12	2.06	0.20
Ridge 1	100	0.98	0.09	1.61	0.16
Ridge 2	20	4.20	0.39	5.60	0.52
Ridge 2	40	2.01	0.19	3.26	0.30
Ridge 2	60	1.33	0.13	2.24	0.22
Ridge 2	80	0.98	0.10	1.64	0.17
Ridge 2	100	0.78	0.08	1.28	0.13
Ridge 3	20	4.50	0.41	6.00	0.54
Ridge 3	40	1.94	0.20	3.15	0.32
Ridge 3	60	1.14	0.12	1.92	0.20
Ridge 3	80	0.79	0.09	1.32	0.15
Ridge 3	100	0.59	0.07	0.97	0.11
Ridge 4	20	3.15	0.32	4.21	0.43
Ridge 4	40	1.88	0.19	3.04	0.31
Ridge 4	60	1.71	0.17	2.88	0.29
Ridge 4	80	1.48	0.15	2.46	0.25

Ridge 4	100	1.38	0.14	2.27	0.23
Ridge 5	20	4.33	0.42	5.77	0.57
Ridge 5	40	1.93	0.19	3.12	0.31
Ridge 5	60	1.44	0.15	2.44	0.25
Ridge 5	80	1.10	0.12	1.83	0.19
Ridge 5	100	0.93	0.10	1.52	0.17
Ridge 6	20	4.68	0.43	6.24	0.58
Ridge 6	40	1.69	0.16	2.73	0.26
Ridge 6	60	1.43	0.14	2.41	0.23
Ridge 6	80	1.08	0.10	1.80	0.17
Ridge 6	100	0.96	0.09	1.58	0.15
Ridge 7	20	4.52	0.45	6.03	0.60
Ridge 7	40	2.60	0.25	4.21	0.40
Ridge 7	60	1.47	0.14	2.48	0.23
Ridge 7	80	1.08	0.10	1.79	0.16
Ridge 7	100	0.80	0.07	1.31	0.12
Ridge 8	20	3.42	0.35	4.56	0.46
Ridge 8	40	2.58	0.24	4.18	0.39
Ridge 8	60	1.62	0.16	2.73	0.27
Ridge 8	80	1.30	0.13	2.17	0.22
Ridge 8	100	1.03	0.11	1.69	0.17
Ridge 9	20	3.44	0.33	4.58	0.45
Ridge 9	40	1.70	0.17	2.74	0.27

Ridge 9	60	1.27	0.13	2.15	0.22
Ridge 9	80	0.99	0.10	1.65	0.17
Ridge 9	100	0.84	0.09	1.38	0.15
Ridge 10	20	3.99	0.38	5.32	0.50
Ridge 10	40	1.80	0.17	2.92	0.27
Ridge 10	60	1.71	0.16	2.89	0.28
Ridge 10	80	1.42	0.14	2.36	0.23
Ridge 10	100	1.34	0.13	2.21	0.21
Shoulder 1	20	3.02	0.30	4.50	0.45
Shoulder 1	40	1.67	0.16	2.45	0.23
Shoulder 1	60	1.33	0.13	2.06	0.21
Shoulder 1	80	1.08	0.11	1.72	0.17
Shoulder 1	100	0.95	0.10	1.54	0.16
Shoulder 2	20	2.73	0.29	4.07	0.43
Shoulder 2	40	1.66	0.17	2.42	0.25
Shoulder 2	60	1.16	0.13	1.80	0.20
Shoulder 2	80	0.93	0.10	1.47	0.16
Shoulder 2	100	0.77	0.09	1.24	0.14
Shoulder 3	20	2.77	0.27	4.13	0.40
Shoulder 3	40	1.52	0.15	2.22	0.22
Shoulder 3	60	0.94	0.10	1.45	0.15
Shoulder 3	80	0.70	0.08	1.11	0.12
Shoulder 3	100	0.54	0.06	0.88	0.10

Shoulder 4	20	2.96	0.29	4.41	0.43
Shoulder 4	40	1.81	0.19	2.65	0.28
Shoulder 4	60	1.48	0.15	2.29	0.24
Shoulder 4	80	1.24	0.13	1.97	0.21
Shoulder 4	100	1.10	0.12	1.79	0.19
Shoulder 5	20	3.33	0.33	4.96	0.50
Shoulder 5	40	1.83	0.17	2.68	0.25
Shoulder 5	60	1.17	0.12	1.82	0.18
Shoulder 5	80	0.89	0.09	1.41	0.14
Shoulder 5	100	0.70	0.07	1.13	0.12
Shoulder 6	20	3.14	0.32	4.68	0.47
Shoulder 6	40	1.42	0.14	2.08	0.21
Shoulder 6	60	1.58	0.15	2.44	0.23
Shoulder 6	80	1.37	0.13	2.18	0.21
Shoulder 6	100	1.40	0.13	2.27	0.21
Shoulder 7	20	2.61	0.26	3.90	0.38
Shoulder 7	40	1.62	0.16	2.36	0.23
Shoulder 7	60	1.12	0.11	1.74	0.17
Shoulder 7	80	0.89	0.08	1.41	0.13
Shoulder 7	100	0.73	0.07	1.19	0.11
Shoulder 8	20	2.43	0.25	3.62	0.37
Shoulder 8	40	1.71	0.17	2.50	0.24
Shoulder 8	60	1.12	0.11	1.74	0.17

Shoulder 8	80	0.90	0.09	1.43	0.14
Shoulder 8	100	0.73	0.07	1.18	0.12
Shoulder 9	20	3.44	0.31	5.13	0.46
Shoulder 9	40	1.77	0.17	2.58	0.25
Shoulder 9	60	1.29	0.12	2.00	0.19
Shoulder 9	80	1.00	0.10	1.59	0.15
Shoulder 9	100	0.84	0.08	1.36	0.13
Shoulder 10	20	2.27	0.24	3.38	0.36
Shoulder 10	40	1.59	0.17	2.33	0.25
Shoulder 10	60	1.13	0.12	1.75	0.19
Shoulder 10	80	0.93	0.10	1.47	0.16
Shoulder 10	100	0.77	0.09	1.26	0.14
Slope 1	20	3.00	0.23	4.51	0.34
Slope 1	40	0.77	0.07	1.34	0.12
Slope 1	60	0.43	0.01	0.75	0.01
Slope 1	80	0.27	0.00	0.46	0.01
Slope 1	100	0.19	0.00	0.33	0.00
Slope 2	20	4.39	0.33	6.61	0.49
Slope 2	40	1.30	0.12	2.27	0.22
Slope 2	60	0.67	0.05	1.16	0.09
Slope 2	80	0.41	0.03	0.71	0.06
Slope 2	100	0.28	0.02	0.49	0.04
Slope 3	20	2.78	0.25	4.19	0.38

Slope 3	40	0.91	0.09	1.59	0.16
Slope 3	60	0.99	0.08	1.73	0.15
Slope 3	80	0.80	0.06	1.40	0.11
Slope 3	100	0.80	0.06	1.40	0.10
Slope 4	20	2.46	0.20	3.70	0.31
Slope 4	40	1.15	0.11	2.02	0.19
Slope 4	60	0.70	0.07	1.22	0.11
Slope 4	80	0.50	0.05	0.88	0.08
Slope 4	100	0.38	0.04	0.67	0.06
Slope 5	20	3.08	0.28	4.63	0.41
Slope 5	40	1.36	0.14	2.38	0.24
Slope 5	60	0.96	0.09	1.67	0.16
Slope 5	80	0.71	0.07	1.24	0.12
Slope 5	100	0.58	0.06	1.02	0.10
Slope 6	20	3.04	0.25	4.58	0.38
Slope 6	40	0.75	0.07	1.31	0.12
Slope 6	60	0.56	0.05	0.97	0.09
Slope 6	80	0.37	0.04	0.65	0.07
Slope 6	100	0.31	0.03	0.54	0.06
Slope 7	20	1.56	0.15	2.35	0.23
Slope 7	40	0.72	0.04	1.26	0.07
Slope 7	60	0.74	0.04	1.30	0.08
Slope 7	80	0.64	0.04	1.11	0.06

Slope 7	100	0.63	0.04	1.10	0.06
Slope 8	20	2.36	0.21	3.55	0.32
Slope 8	40	1.14	0.11	2.00	0.19
Slope 8	60	0.75	0.07	1.30	0.12
Slope 8	80	0.55	0.05	0.96	0.09
Slope 8	100	0.44	0.04	0.76	0.07
Slope 9	20	2.65	0.23	3.99	0.35
Slope 9	40	0.96	0.10	1.68	0.18
Slope 9	60	0.55	0.06	0.95	0.10
Slope 9	80	0.36	0.04	0.63	0.07
Slope 9	100	0.26	0.03	0.46	0.05
Slope 10	20	3.26	0.27	4.90	0.40
Slope 10	40	1.01	0.10	1.76	0.18
Slope 10	60	0.58	0.05	1.01	0.09
Slope 10	80	0.37	0.04	0.65	0.06
Slope 10	100	0.27	0.03	0.47	0.04

Table A3. Mean values with standard deviations in parentheses of soil bulk density along the toposequence and with depth.

Transect	Depth (cm)	Bulk Density (g/cm3)
Ridge	0-20	0.67 (0.08)
	20-40	0.81 (0.03)
	40-60	0.84 (0.01)
	60-80	0.83 (0.06)
	80-100	0.82 (0.11)
Shoulder	0-20	0.75 (0.03)
	20-40	0.73 (0.02)
	40-60	0.78 (0.01)
	60-80	0.80 (0.02)
	80-100	0.81 (0.03)
Slope	0-20	0.75 (0.06)
	20-40	0.88 (0.02)
	40-60	0.87 (0.01)
	60-80	0.87 (0.02)
	80-100	0.87 (0.03)

Table A4. Soil chemical and spatial data for the larger landscape sampling sites. Chemical data are from surface soils, 0–10 cm. The length scale for slope angle measurements is 10 m, derived from a digital elevation map of the study site.

Sample ID	Latitude	Longitude	Soil C (%)	Soil N (%)	$\delta^{15}N$ (‰)	Slope angle (°)	Elevation (m)
Slope 01	8°24'17.6"N	83°20'1.4"W	2.55	0.26	5.65	13	36
Slope 02	8°24'18.4"N	83°20'1.7"W	4.24	0.38	5.63	17	38
Slope 03	8°24'19.7"N	83°20'1.6"W	4.54	0.33	5.83	13	49
Slope 04	8°24'20.1"N	83°20'0.1"W	3.57	0.29	4.91	33	40
Slope 05	8°24'21.2"N	83°19'59.7"W	5.47	0.44	5.05	30	38
Slope 06	8°24'20.2"N	83°19'59.7"W	4.50	0.34	4.18	31	38
Slope 07	8°24'19.9"N	83°19'59.7"W	3.66	0.31	5.08	27	32
Slope 08	8°24'22.1"N	83°20'2.1"W	3.73	0.32	5.54	14	52
Slope 09	8°24'23.7"N	83°20'2.6"W	3.67	0.31	5.32	31	38
Slope 10	8°24'24.1"N	83°20'3.5"W	3.93	0.34	5.24	21	32
Slope 11	8°24'23"N	83°20'3.1"W	3.21	0.25	4.45	24	32
Slope 12	8°24'26.3"N	83°19'56.5"W	5.09	0.41	5.53	7	78
Slope 13	8°24'28.1"N	83°19'56.1"W	5.50	0.49	5.96	11	85
Slope 14	8°24'29.1"N	83°19'56.3"W	4.21	0.38	5.59	11	87

Slope 15	8°24'30.3"N	83°19'54"W	4.64	0.45	6.57	9	103
Slope 16	8°24'34.4"N	83°19'54.3"W	4.99	0.48	6.45	12	113
Slope 17	8°24'33.3"N	83°19'53.6"W	4.89	0.46	6.02	10	112
Slope 18	8°24'31.5"N	83°19'55.5"W	5.85	0.52	5.49	15	102
Slope 19	8°24'25.6"N	83°19'59"W	5.53	0.50	5.73	7	69
Slope 20	8°24'25.4"N	83°19'59.7"W	3.47	0.33	6.57	12	67
Slope 21	8°24'25.2"N	83°20'1.4"W	4.76	0.37	5.11	25	49
Slope 22	8°24'16.8"N	83°19'59.3"W	2.21	0.23	5.60	22	30
Slope 23	8°24'17.4"N	83°19'58.3"W	5.11	0.39	4.40	26	45
Slope 24	8°24'17.8"N	83°19'57.9"W	4.35	0.36	4.61	24	49
Slope 25	8°24'35.7"N	83°19'50.3"W	4.81	0.42	5.27	10	137
Slope 26	8°24'36.4"N	83°19'49.2"W	2.73	0.27	3.79	35	135

Table A5. Parameters used in ^{15}N mass balance models and their sources.

Parameter	Value	Source
a_f	0.993	Solved for using observed isotope data from Piro, assuming flattest parts of the landscape have no non-fractionating N loss ($k_E/k_{ex} = 0$)
a_E	1	Definition of non-fractionating loss
N_s (kg N ha^{-1})		
-scenario A	2,700	Mean values from 0-10 cm surface soils, Piro toposequence
-other scenarios	3,200 - 2,000	Linear decline in soil N content with increasing slope angle, based on top 10 cm soil N contents across Piro toposequence
R_A	0.0036765	Accepted value for the atmosphere
R_r	0.003680 - 0.003699	Based on reported range of $\delta^{15}N$ values for sedimentary rocks, approximately 1- 6 ‰ (Holloway and Dahlgren 2002)
I (kg N ha^{-1} yr^{-1})	9.7	Site-based estimate of BNF (Sullivan et al. 2014, 5.7 kg N ha^{-1} yr^{-1}) + modeled N deposition (Detner et al. 2006 4.0 kg N ha^{-1} yr^{-1})

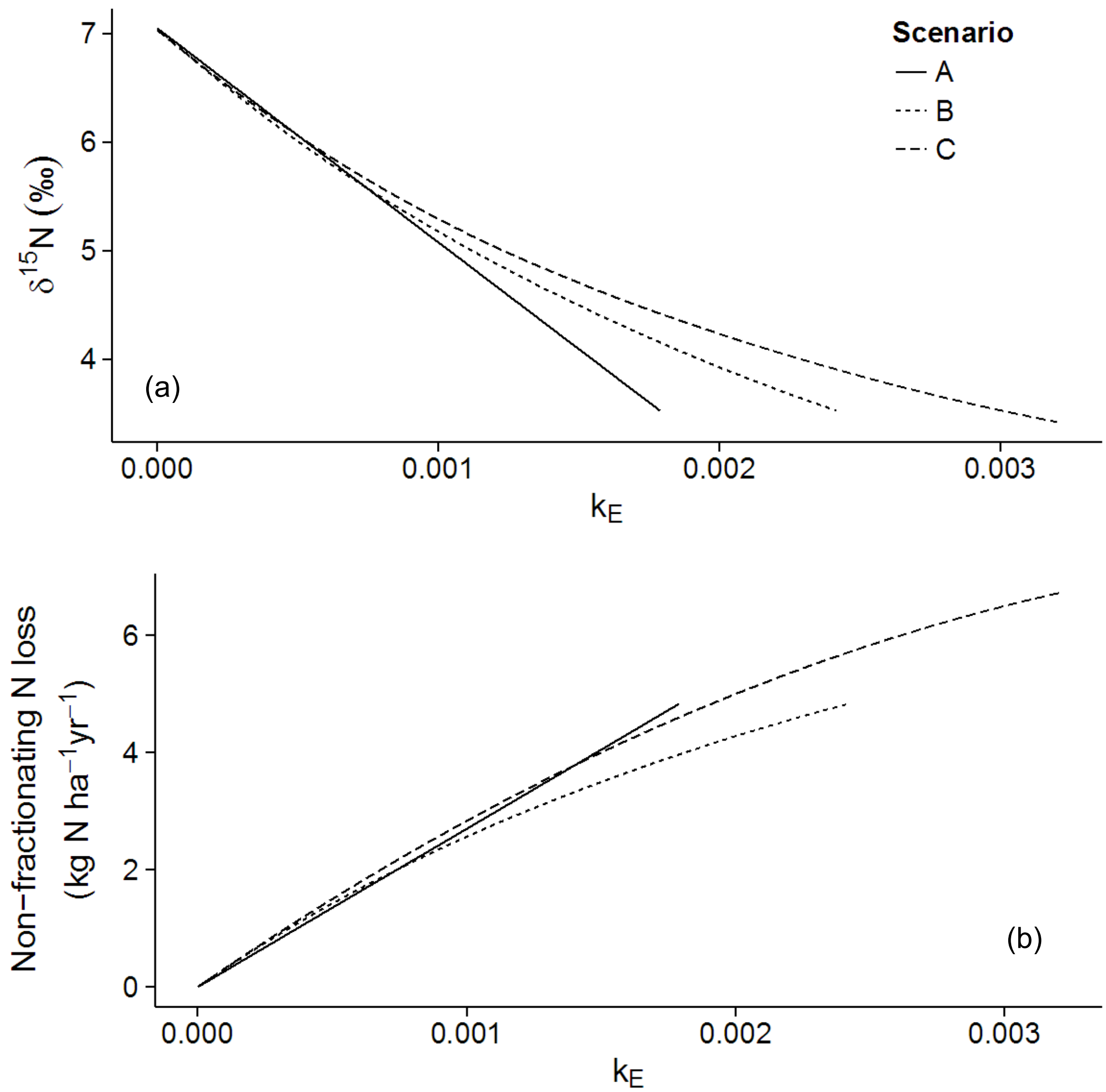

FIG. A1. Modeled relationships between k_E and soil $\delta^{15}N$ values (a) and k_E and non-fractionating N losses (b) for three different scenarios, described in the above section on *nitrogen isotope mass balance modeling*.

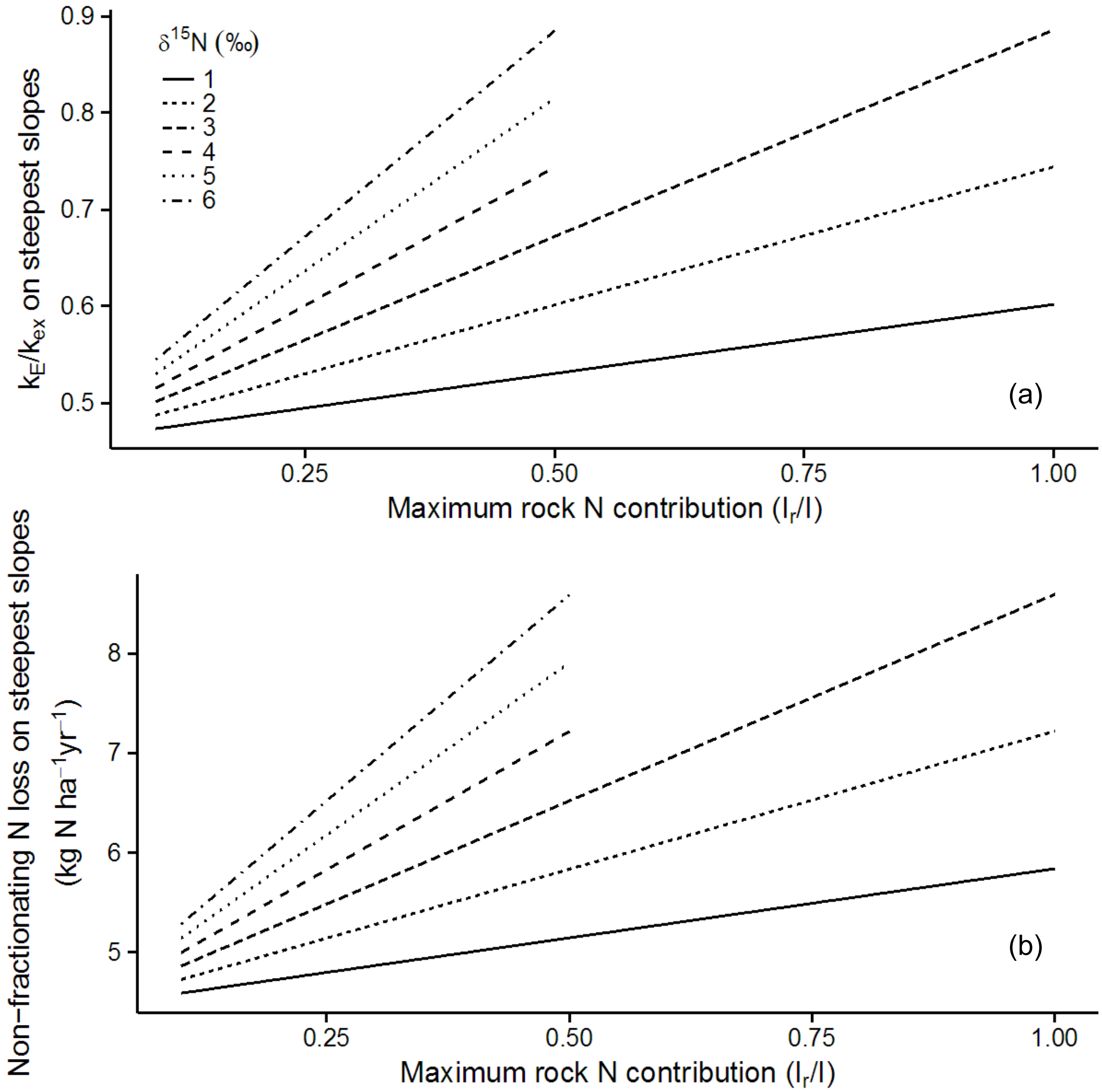

FIG. A2. Modeled relationships between the maximum contribution of bedrock N to total N inputs on steep slopes and the increase in k_E/k_{ex} (a) and non-fractionating N losses (b) required to achieve observed isotope values under these conditions and across a range of soil δ^{15}N values.